Full Wave Analysis of a Dual-Frequency Printed Slot Antenna with Microstrip Feed

R. Hasse[1, *], K. Naishadham[1], W. Hunsicker[1], M. Tentzeris[2], and T. Wu[2]

[1] Georgia Tech Research Institute
Georgia Institute of Technology, Atlanta, Georgia 30332-0858
roger.hasse@gtri.gatech.edu

[2] Department of Electrical and Computer Engineering
Georgia Institute of Technology, Atlanta, Georgia 30332-0250

INTRODUCTION

Coupled microstrip-slotline antenna designs employ a microstrip feed line to excite a linear or ring slot in the ground plane of the structure via electromagnetic coupling, and such designs have proven successful in achieving dual-frequency operation with wide bandwidths [1, 2]. A dual-frequency printed antenna design of interest to the authors for its potential use as an array unit cell was published in the literature as an experimental study [3]. The design consists of a linear slot embedded inside the metallic patch formed by a square ring slot in the ground plane of a microstrip line. Both slots are coupled to a 50 Ω feed line through parallel alignment on one side of the ring slot at fixed offset. The ring slot excites the first resonant mode, and electromagnetic coupling between both slots excites the second resonant mode. The layout for the printed slot antenna in the x-y plane is shown in Figure 1. This paper investigates the simulated performance of the antenna with a linear slot length of $L = 30$ mm, with a view of understanding the physical basis of electromagnetic coupling from the microstrip feed line to the two slot elements. Full-wave analysis reveals the existence of two significant anti-resonant modes which bound the second resonance. These modes, which were not reported earlier, are generated when the linear slot length approaches one-quarter and one-half free-space wavelengths, and are correlated in this paper with standing waves of magnetic current on the linear slot. The far-field radiation patterns and total gains are reported and compared to the results from the experimental study [3]. An equivalent circuit model of the dual-frequency printed slot antenna is presently under investigation.

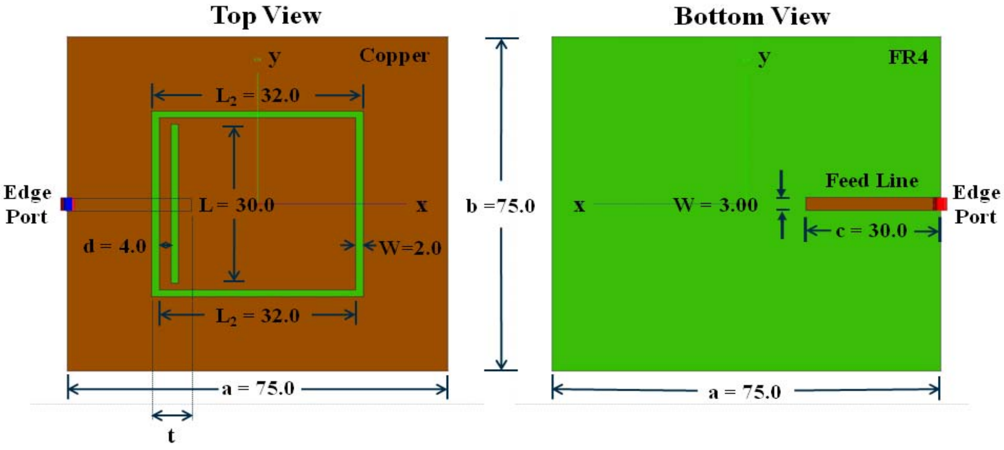

Figure 1. Design layout for the dual-frequency printed slot antenna (dimensions in mm).

ANTENNA MODEL

978-1-4244-4968-2/10/$25.00 ©2010 IEEE

The geometry of the slot antenna is analyzed using the FEKO 3-D electromagnetic solver [4]. The antenna is constructed on FR4 substrate of thickness $h = 1.6$ mm, permittivity $\varepsilon_r = 4.4$, and loss tangent $\tan \delta = 0.02$. The ground plane dimensions are 75 mm × 75 mm. A linear slot of length $L = 30$ mm is embedded into the inner patch bounded by a square ring slot with outer and inner perimeter dimensions of $L_1 = 36$ mm and $L_2 = 32$ mm, respectively. The width of each slot is $W = 2$ mm and their offset is $d = 4$ mm. The tuning stub length measured from the outer edge of the ring slot to the open-end of the microstrip line was fixed to $t = 10.5$ mm. The skin effect approximation is applied to all copper surfaces of thickness 17 μm, and the inner conducting patch modeled as a floating ground. An edge port drives the antenna at 1 V excitation with 20 mW power. The feed line width is fixed to $W = 3$ mm for a 50 Ω impedance (feed width not reported in [3]). The Surface Equivalence Principle (MoM) is used in modeling the performance with adaptive frequency sweeps from 1 to 4 GHz. Electric and magnetic surface currents and far-field patterns are then calculated at each resonant-band center frequency.

SIMULATION RESULTS

The simulated return loss and input impedance for the dual-slot antenna is shown in Figure 2. The first anti-resonant mode ($|Z_{in}| = 422\ \Omega$ at 2.331 GHz) corresponds to $\lambda_0/4 = 32$ mm, where λ_0 corresponds to the free space wavelength. The linear slot length is very close to $\lambda_0/4$ at this frequency, and generates an asymmetrical shoulder in the return loss response. The second anti-resonant mode ($|Z_{in}| = 204\ \Omega$ at 3.518 GHz) corresponds to $\lambda_0/2 = 42$ mm. The linear slot length equals $0.71 \times \lambda_0/2$ at this frequency, and smoothly perturbs the return loss response. The simulated resonant-band center frequencies are 1.491 GHz with a RL of -19.8 dB, and 2.875 GHz with RL at -39.9 dB.

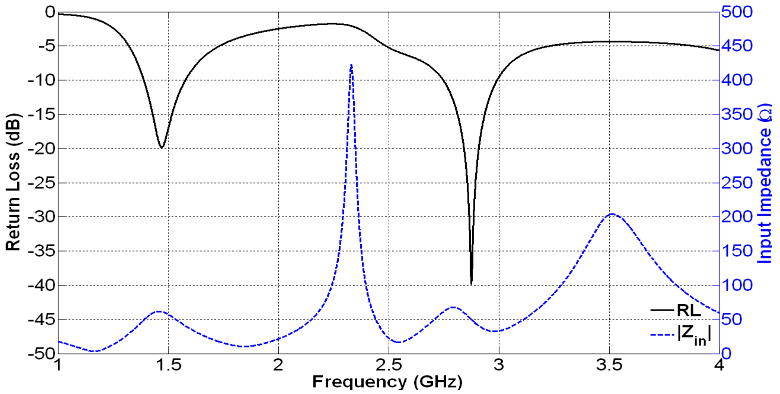

Figure 2. Simulated return loss and input impedance for printed dual-slot antenna.

Disagreement with the resonant frequencies of 1.570 GHz and 2.916 GHz reported in [3] is likely due to manufacturing tolerances in the fabricated antennas. In addition, the model presented here does not account for coaxial-to-microstrip losses in the SMA connector. Closed-form expressions [5] were used to calculate the guided-slot wavelength λ_S on the square ring slot. The computed free-space and ring-slot wavelengths at 1.491 GHz are 201.2 and 159.2 mm, respectively. Thus, $\lambda_S = 0.79\lambda_0$ on the square ring slot. However, the slot wavelength of the first resonant frequency does not correspond to the mean radius of the square ring slot ($r = s \times \sqrt{2}/2 = 24$ mm) as erroneously reported in [3], but rather is slightly larger than the mean slot circumference ($4s = 136$ mm), where $s = 34$ mm is the mean side length of the ring slot.

The electric and magnetic surface current distributions for the first *anti-resonant* mode are shown in Figure 3. The electric surface currents are high at the linear slot ends, and repulsed by currents on the ring slot's inner edge. A standing wave of magnetic current can be seen on the linear slot length, indicating phase inversion at the slot ends.

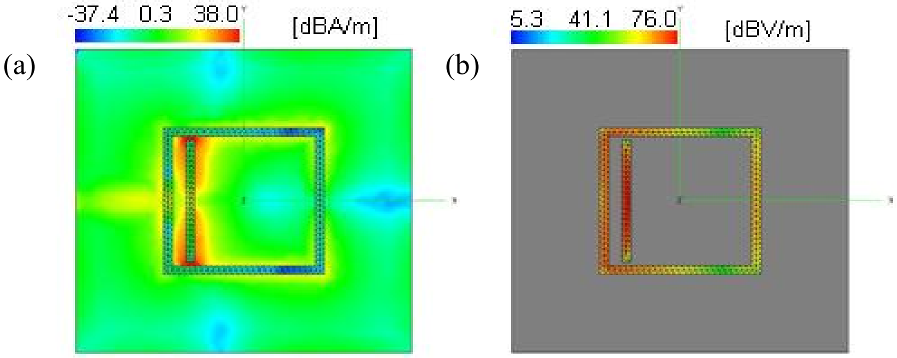

Figure 3. Simulated (a) electric surface current and (b) magnetic surface current distributions for the printed slot antenna at first anti-resonant mode (2.331 GHz).

The electric and magnetic surface current distributions for the first and second *resonant* modes are shown in Figure 4. Only the ring slot is excited at the first resonant frequency as indicated by the strong distribution of electric surface current along its perimeter. At the second resonant mode both slots are radiating, as indicated by the electric surface currents flowing around the perimeters of each slot. Standing waves of magnetic current are also seen on each side of the square ring slot and on the embedded linear slot.

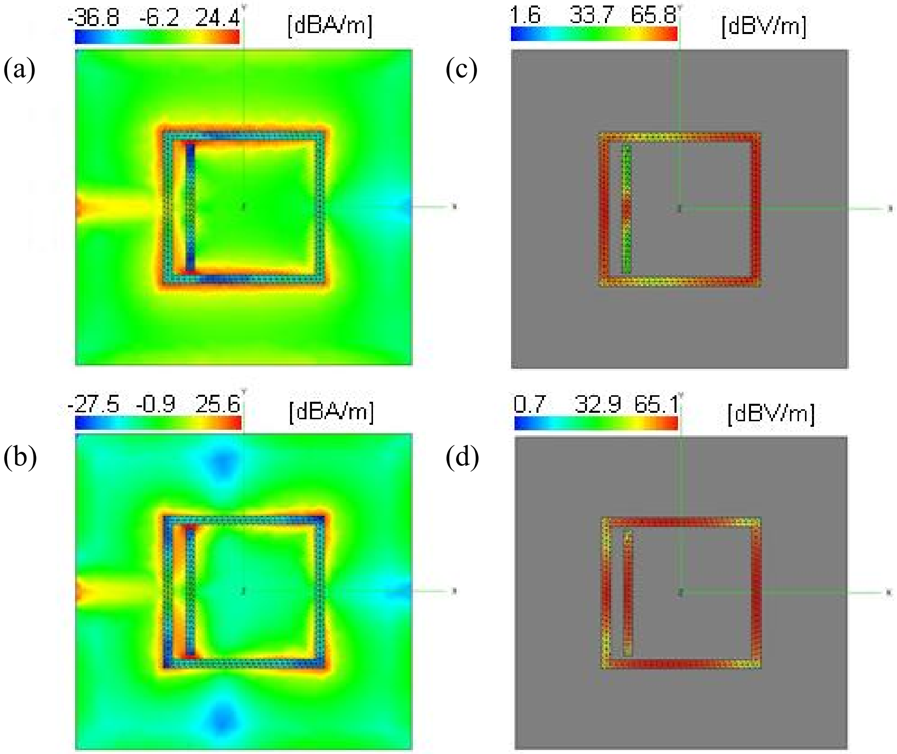

Figure 4. Simulated (a), (b) electric surface current and (c), (d) magnetic surface current distributions for the printed slot antenna at *resonant* modes 1.491 GHz and 2.875 GHz.

The simulated directive gain patterns (normalized) in three planes are shown for each resonant frequency in Figure 5. The total gains are 3.65 dB (1.491 GHz) and 2.59 dB (2.875 GHz), respectively. The first resonant mode is ≅ 1 dB lower in gain than reported in [3], perhaps due to radiation from surface currents along the feed cable during measurement. The radiation patterns are verified as broadside and bidirectional. Large cross-polarization in the *y-z* plane for the second *resonant* mode is also verified.

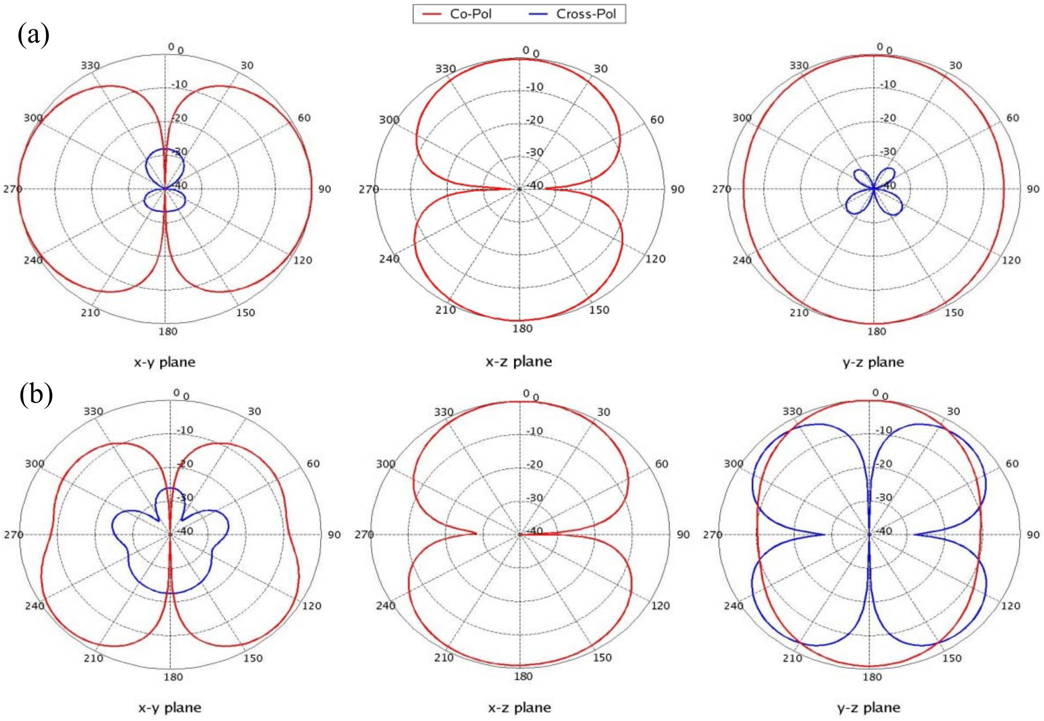

Figure 5. Simulated directive gain patterns in three planes at (a) 1.491 and (b) 2.875 GHz.

CONCLUSION

The performance of a dual-frequency printed slot antenna design with linear slot length *L* = 30 mm has been verified using full-wave analysis. Anti-resonant modes are generated when the linear slot length approaches one-quarter and one-half free-space wavelengths.

REFERENCES

[1] H. Tehrani and K. Chang, ‘Multifrequency operation of microstrip-fed slot-ring antennas on thin low-dielectric permittivity substrates,’ *IEEE Trans. Antennas Propagat.*, vol. 50, pp. 1299-1308, Sep. 2002.

[2] J.Y. Sze, C.G. Hsu, and S.C. Hsu, ‘Design of a Compact Dual-Band Annular-Ring Slot Antenna,’ *IEEE Ant. and Wireless Propagat. Letters*, vol. 6, pp. 423-426, June 2007.

[3] S.Y. Lin and K.L. Wong, ‘A dual-frequency microstrip-line-fed printed slot antenna,’ *Microw. Opt. Technol. Lett.*, vol. 28, pp. 373-375, Mar. 2001.

[4] FEKO Suite 5.5, EM Software and Systems–S.A. (Pty) Ltd, 32 Techno Avenue, Technopark, Stellenbosch, 7600, South Africa, 1999-2009, http://www.feko.info.

[5] R. Janaswamy and D.H. Schaubert, “Characteristic Impedance of a Wide Slotline on Low-Permittivity Substrates,” *IEEE Trans.*, vol. MTT-34, 1986, pp.900-902.